NANO · MICRO small

Supporting Information

for *Small*, DOI 10.1002/smll.202412784

Layer-by-Layer Assembly of Graphene Oxide and Silver Nanowire Thin Films with Interdigitated Nanostructure in Dendrite Suppressions of Li-Metal Batteries

Sojeong Won, Arum Jung, Kyeong Yeon Lim, Jinhan Cho, Jeong Gon Son, Hee-Dae Lim and Bongjun Yeom**

Supporting Information

Layer-by-Layer Assembly of Graphene Oxide and Silver Nanowire Thin Films with Interdigitated Nanostructure in Dendrite Suppressions of Li-metal Batteries

Sojeong Won, Arum Jung, Kyeong Yeon Lim, Jinhan Cho, Jeong Gon Son,

Hee-Dae Lim, and Bongjun Yeom**

S. Won, A. Jung, K. Y. Lim, H. -D. Lim, B. Yeom
Department of Chemical Engineering
Hanyang University
Seoul 04763, Republic of Korea
Email: hdlim@hanyang.ac.kr; byeom@hanyang.ac.kr

J. Cho
Department of Chemical and Biological Engineering
Korea University
Seoul 02841, Republic of Korea

J. Cho, J. G. Son
KU-KIST Graduate School of Converging Science and Technology
Korea University
Seoul 02841, Republic of Korea

J. Cho, J. G. Son
Soft Hybrid Materials Research Center
Korea Institute of Science and Technology (KIST)
Seoul 02792, Republic of Korea

H. -D. Lim, B. Yeom
Department of Battery Engineering
Hanyang University
Seoul 04763, Republic of Korea

Experimental section

Material Preparations

Graphene oxide powder (GO-V50) was purchased from Standard Graphene. Polyethyleneimine (PEI, branched, M_w = 50,000–100,000, 30% w/w aqueous solution) was purchased from Thermofisher Scientific. Silver nitrate (≥99%), poly(vinylpyrrolidone) (PVP, M_w ~ 55,000), glycerol (reagent plus, ≥99%), and sodium chloride (≥99.5%) were purchased from Sigma-Aldrich for AgNW synthesis. Cysteamine (MEA, ~ 95%), 1,2-ethanedithiol (EDT, ≥ 98%), and tris(2-aminoethyl)amine (TREN, 96%) were purchased from Sigma-Aldrich for LbL assembly. Li-metal foil with a thickness of 300 μm was purchased from Honjo Metal Co. Ltd. The $LiFePO_4$ was purchased from Xintai Yinhe New Energy Materials Co. Ltd. Carbon black (Super P) was purchased from TIMCAL. Polyvinylidene fluoride (PVDF) was obtained from Kureha Corporation. N-methyl-2-pyrrolidone (NMP) was purchased from Daejung Chemicals. Lithium nitrate ($LiNO_3$, reagent plus) for electrolyte additive was obtained from Sigma-Aldrich. 1,3-dioxolane (DOL)/1,2-dimethoxyethane (DME) (1:1) electrolyte with 1 M LiTFSI was obtained from Dongwha Electrolyte.

Synthesis of AgNWs

AgNWs were synthesized via polyol reduction process adopted from Yang *et al.*[S1] We utilized 5.86 g of PVP as a stabilizer, which was dissolved in 190 ml glycerol at 80 °C. After the reaction vessel was cooled to room temperature, 1.58 g of $AgNO_3$ and a mixture of 10 ml glycerol, 0.5 ml DI water, and 33.5 mg NaCl were sequentially added. The reaction vessel was agitated with an overhead stirrer at 50 rpm, and the temperature was slowly

increased to 210 °C for 20 min. After the AgNW growth reaction, the vessel was cooled to room temperature. For purification, DI water was added to the solution at a ratio of 1:1 and centrifuged at 4000 rpm at 10 °C for 20 min. This process was repeated thrice to obtain the final AgNW dispersed solution

Fabrications of LbL assembled Highly Interdigitated Thin Films for Anodes

Copper foils with a thickness of 10 μm were typically utilized as substrates for coatings of the LbL-assembled thin films for most electrochemical tests. Quartz and Si wafer substrates were utilized for UV-visible spectroscopy and field emission scanning microscopy (FE-SEM), respectively. The substrates were immersed in 0.5 wt% PEI aqueous solutions to deposit PEI pre-layers to increase adhesion. After immersion for 30 min, the pre-layer coated substrates were washed with DI water to remove weakly bound materials from the substrates and dried for the preparations of the GO/AgNW LbL-assembled thin film (GA) coatings. The substrates were sequentially immersed in 0.1 wt% GO, MEA, AgNW, and MEA aqueous solutions to form $(GO/MEA/AgNW/MEA)_1$ LbL films denoted as GA_1. Immersion time was 5 min for each deposition. Washing and drying steps were introduced between each layer deposition. Only for the AgNW depositions, the AgNW dispersion containers with the substrates were shaken by a vortex shaker for homogeneous AgNW depositions.[S2] This process was repeated as the desired number (n) of LbL depositions was achieved for GA_n samples. For GA samples, the top-most depositions were GO layers as represented with notations of $GA_{n.25}$. For control samples, $(AgNW/EDT)_n$ and $(GO/TREN)_n$ LbL thin film were separately prepared in the same manner, as denoted as A_n and G_n samples, respectively. The last layers of A or G samples were AgNW or GO layers, which were denoted as $A_{n.5}$ or $G_{n.5}$ samples, respectively.

Preparation of the Cathodes and the Cells for Electrochemical Tests

To prepare the LFP slurry, LFP powder, carbon black, and PVDF were mixed at a ratio of 8:1:1 in NMP at 80 °C for 6 h. The prepared LFP slurry was bar-coated on the carbon-coated aluminum foil. LFP-coated aluminum foil was pre-dried in a convection oven at 80 °C for 2 h, followed by further heating in a vacuum oven at 120 °C for 24 h to remove the remaining NMP solvent. The LFP cathode was cut into disks with a diameter of 12 mm. The LFP cathode mass loading for the full-cell tests was adjusted to 6–7 mg cm^{-2}.

Morphology and Spectroscopic Characterizations

UV-visible spectra were obtained from a Lambda 365 instrument (PerkinElmer) to examine the LbL deposition behaviors. X-ray photoelectron spectroscopy (XPS) analysis was measured with an XPS spectrometer (NEXSA, Thermo Fisher Scientific Co.) with an Al-Kα X-ray source (hv = 1486.6 eV). The sheet resistances of the samples were measured with a four-point probe (CMT-100S, Advanced Instrument Technology). The surface morphologies of the samples with Li depositions were analyzed by FE-SEM (S-4800, Hitachi). Before imaging the Li deposition behavior, the Li deposited electrodes were washed with DOL/DME (1:1) electrolyte to remove residual salts on the surfaces. Then, the samples were completely dried at 80 °C in a glovebox for 24 h before the imaging. Contact angles were measured with 1 M LiTFSI in DOL/DME (1:1) liquid electrolyte droplets by a contact angle analyzer (Phoenix150, S.E.O.).

Electrochemical Characterizations

CR2032 coin cells were assembled in an argon-filled glovebox (Mbraun) with oxygen and humidity concentrations below 0.5 ppm for electrochemical analysis. Celgard 2400 membranes with a diameter of 16 mm were utilized as the separator. For the CE test, Li deposition behavior, and cyclic voltammetry (CV) test, and rate capabilities of half cells, pristine Cu, GA, A, or G samples were utilized as working electrodes, and Li-metals were utilized as counter electrodes for half-cell tests. For the nucleation overpotential tests, 5 different batches of the samples were tested and the representative results were plotted in Figure 4d. The rate capability test was performed after stabilizing SEI formation by one-time Li plating at 0.5 mA cm^{-2}, 4 mAh cm^{-2} and stripping at a cut-off voltage of 1 V. For long-term cycling tests, the symmetric cells were assembled with two electrodes pre-deposited with the desired amounts of Li. The full cells were assembled with the pre-Li-deposited electrodes and LFP cathodes. All electrochemical tests were examined with additions of 100 μl of 1 M LiTFSI in DOL/DME (1:1) electrolyte. In most cases, 1 wt% $LiNO_3$ additive was added except otherwise stated. Electrochemical impedance spectroscopy (EIS) analysis was performed with a WonATech ZIVE SP1 in the frequency range of 1 MHz–0.1 Hz. It was assembled with Li@current collector (CC)/Li cells, where Li@CC indicates pre-depositions of Li on the current collectors. Li pre-depositions were performed at a current density of 0.5 mA cm^{-2} with varied capacities of 0.2–4 mAh cm^{-2} on the pristine Cu, GA, A, and G samples. To obtain charge-transfer resistance (R_{ct}), the Nyquist plots were fitted to an equivalent circuit model with WonATech ZMAN software. As indicated in the main texts, symmetric cell tests to evaluate long-term cycling stability were performed under various conditions. The rate performances of LFP/Li@CC full cells were examined by step-wise increase of the C-rate from 0.1 to 0.5, 1, 2, 5 C and return to 0.1 C in the voltage window of 2.7–4.0 V. The LFP/Li@CC full cells for longer-term cycle tests proceeded under conditions

of 1 C and 3 C in the same voltage window. All cell tests were performed with a battery cycler (WonATech, WBCS3000) at a constant temperature of 30 °C.

Table S1. Summary of recent studies on Li-metal anodes with lithiophilically modified Cu foils. Full-cell test results obtained with Li pre-deposited anodes and LFP cathodes are selected for comparison. N/P ratios are calculated based on Li pre-deposition capacities and cathode-mass loadings in the corresponding full-cell tests. The studies are listed in increasing order of N/P ratio.

	Anode	Pre-deposited Li with capacity [mAh cm–2]	Cathode mass loading [mg cm^{-2}]	N/P ratio	C-rate & No. of cycles (cut off 80%)	Ref.
This work	$GA_{9.25}$	2	6.5	1.81	1 C / 255 3 C / 250	This work
			10	1.18	1 C / 125	
		4	7	3.36	1 C / 430 3 C / 240	
1	Vertically aligned MXene	2	10.6	1.11	0.5 C / 300	Q. Chen *et al, Adv. Energy Mater.* 2022, 12, 2200072[S3]
2	MgF_2/Au	3	12	1.5	0.5 C / 400	J. Jiang et al, Energy Storage Mater. 2023, 54, 885[S4]
			3	5.9	1 C / 450	
3	Yolk-shell SiO_x/C@N/S-doped C	3.2	10.5	1.79	1 C / 350	R. He et al, Adv. Energy Mater. 2023, 13, 2204075[S5]
4	MgF2- N doped graphene like hollow nanospheres	5	6	4.9	0.5 C / 550 1 C / 1000 (cut off 65.9%)	S. Li et al, Adv. Mater. 2022, 34, 2201801[S6]
5	GO-Zn	10	11.5	5.12	1 C / 100	J. Ma et al, Energy Storage Mater. 2023, 56, 572[S7]
6	Vertically aligned Nickel-catecholate	5	5	5.88	0.5 C / 150	Y. Jin et al, Adv. Funct. Mater. 2024, 34, 2310097[S8]
7	Ag nanoparticles	10	7	8.4	1 C / 200	Z. Hou et al, ACS Appl. Mater. Interfaces. 2019, 11, 8148[S9]
8	N-doped carbon macroporous fibers-AgNP	6	4	8.82	1 C / 250	Y. Fang et al, Sci. Adv. 2021, 7, eabg3626[S10]
9	Hollow N, O co-doped carbon nanosphere	6	3.6	9.8	0.5 C / 200	C. Gao et al, Chem. Eng. J. 2021, 412, 128721[S11]
10	Zn-MXene	5	1	29.4	10 C / 500	J. Gu et al, ACS Nano. 2020, 14, 891[S12]

Table S2. Deconvolution of XPS C 1s peaks in pristine GO and $GA_{9.25}$.

		O-C=O	C=O	C-O-C	C-N	C-S	C-O	C-C	C=C	C-O/ C-O-C
GO	Peak position (eV)	288.3	287.1	286.5	-	-	285.5	284.5	283.1	0.34
	Peak area (%)	6.7	8.4	22.8	-	-	7.7	36.1	18.4	
$GA_{9.25}$	Peak position (eV)	288.5	287.2	286.9	286.4	286.2	285.8	284.7	284.2	0.56
	Peak area (%)	5.2	13.5	21.7	3.1	2.3	12.2	31.2	10.8	

Table S3. Sheet resistance of samples coated on Cu foil

	Sheet resistance [ohm sq^{-1}]
Cu foil	1.72×10^{-3}
$G_{9.5}$	1.55×10^{5}
$A_{9.5}$	1.77×10^{-3}
$GA_{9.25}$	2.16×10^{-1}

Table S4. Interfacial resistance of EIS data for Cu, $G_{9.5}$, $A_{9.5}$, and $GA_{9.25}$ at before cycling, 10 cycles, and 50 cycles.

	R_{int} [Ω]		
	Before cycling	10 cycles	50 cycles
Cu	384.0	53.3	55.7
$G_{9.5}$	1387.5	35.5	41.7
$A_{9.5}$	168.9	12.4	59.6
$GA_{9.25}$	249.7	10.1	15.7

Table S5. Sheet resistance of $GA_{n.25}$ coated on glass.

	Sheet resistance [ohm sq^{-1}]
$GA_{1.25}$	66.9×10^3
$GA_{5.25}$	54.2×10^3
$GA_{9.25}$	6.4×10^3
$GA_{15.25}$	11.4×10^3

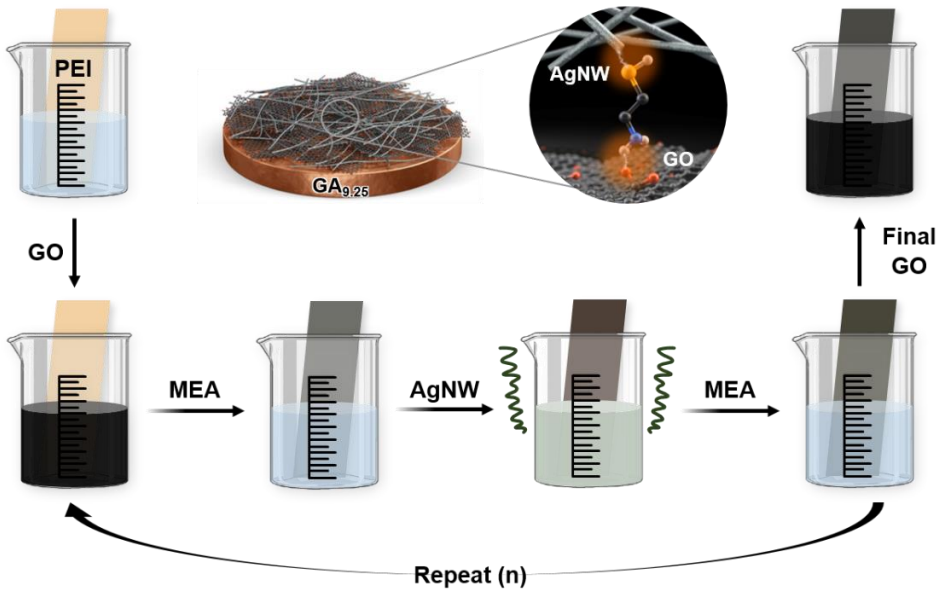

Figure S1. Schematic of layer-by-layer self-assembly process of $GA_{n.25}$.

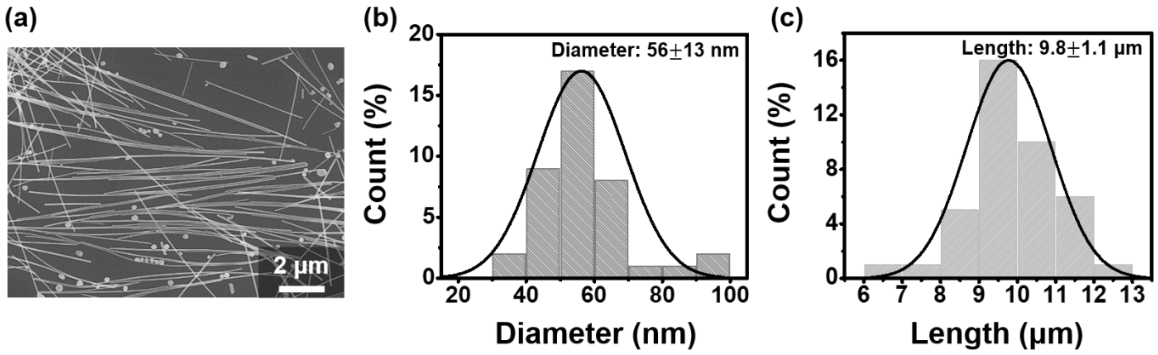

Figure S2. (a) FE-SEM of AgNWs dispersion. Typical SEM and TEM size distributions of (b) diameter and (c) length of silver nanowires. Average diameters and lengths were obtained from fittings of normal distributions.

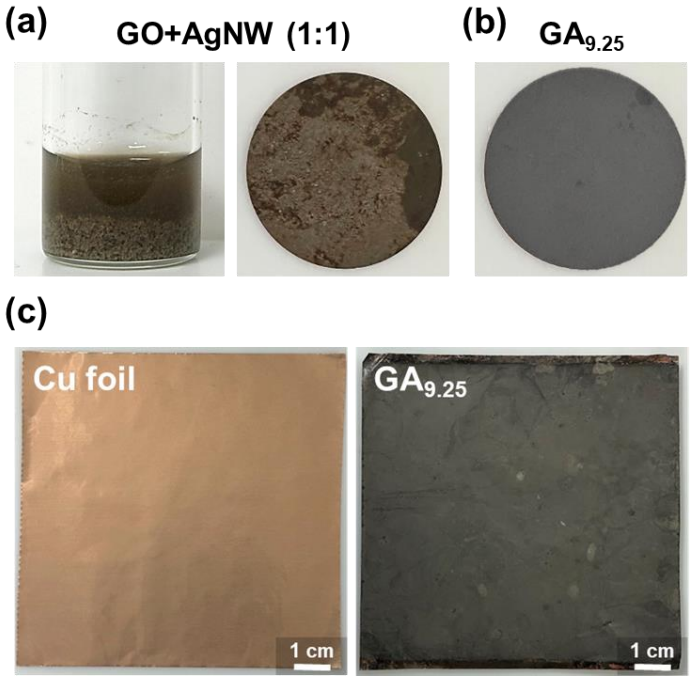

Figure S3. Photographs of solutions after simply mixing GO & AgNW and coated Cu foil (a) GO+AgNW (1:1), (b) $GA_{9.25}$ and (c) Photographs of Cu foil and $GA_{9.25}$ films fabricated in a scalable size of 8.5 cm × 8.5 cm.

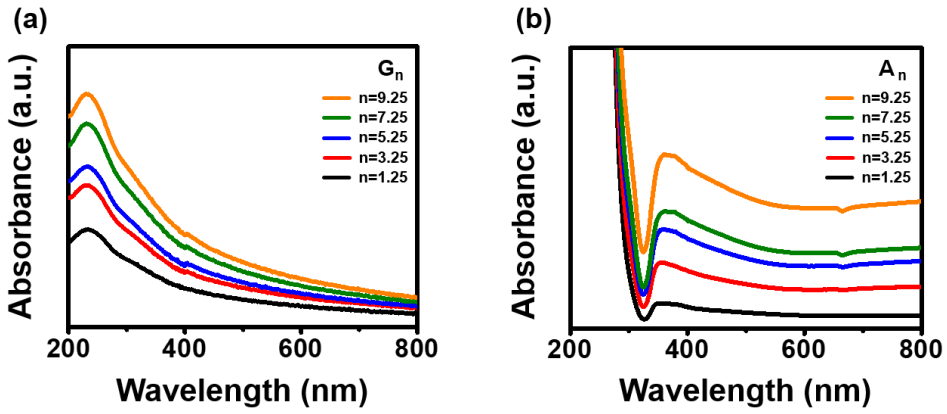

Figure S4. UV-vis absorbance spectra of (a) G_n, and (b) A_n.

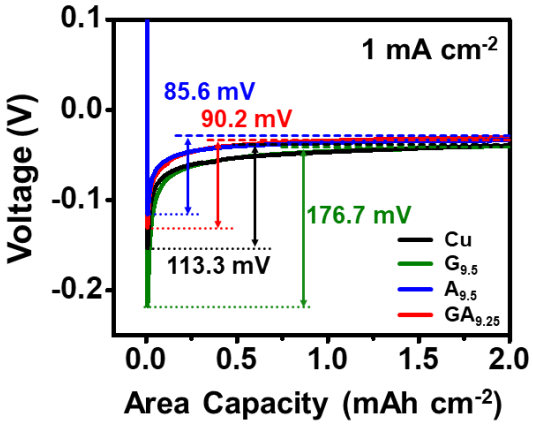

Figure S5. Voltage-capacity profiles of Cu, $G_{9.5}$, $A_{9.5}$, and $GA_{9.25}$. 1 M LiTFSI in DOL/DME (1:1) electrolytes with 1 wt% LiNO3 additive at 1 mA cm^{-2}.

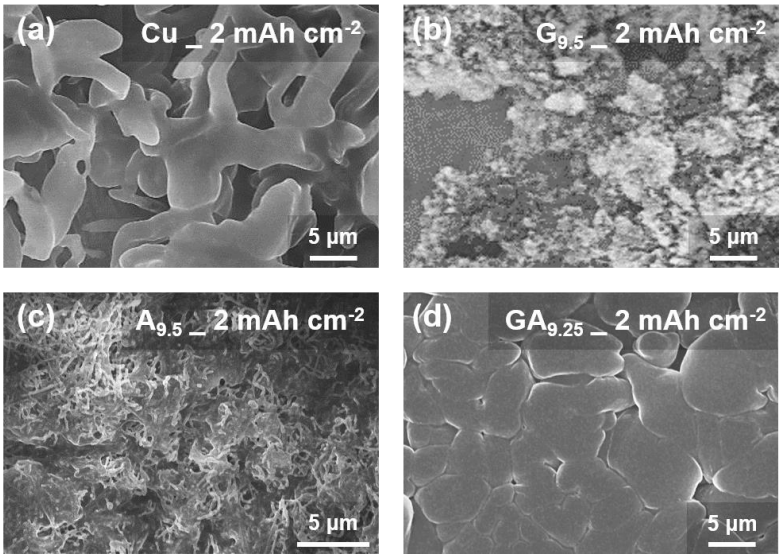

Figure S6. FE-SEM top images of (a) Cu, (b) $G_{9.5}$, (c) $A_{9.5}$ and (d) $GA_{9.25}$ after Li plating at 0.5 mA cm^{-2}, 2 mAh cm^{-2}.

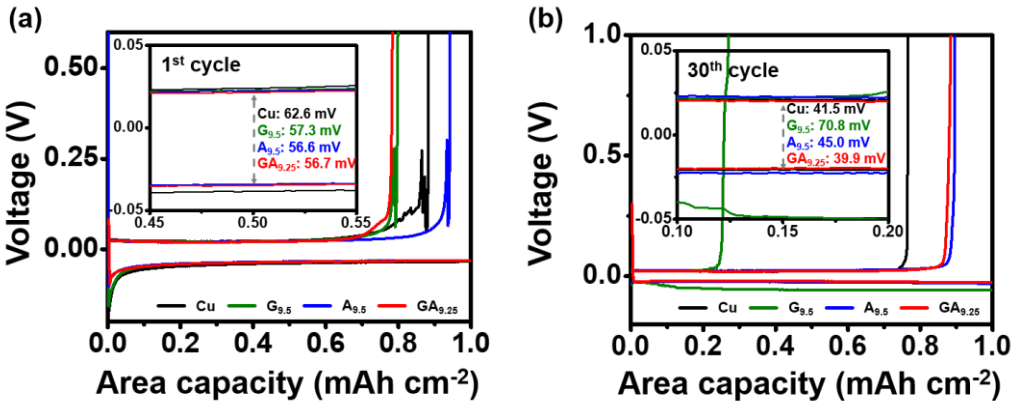

Figure S7. Electrochemical graph of Li-metal plating/stripping curves for Cu, $G_{9.5}$, $A_{9.5}$, and $GA_{9.25}$ after (a) 1st and (b) 30th cycles without $LiNO_3$ additives in electrolytes (inset: enlarged scale of electrochemical graphs).

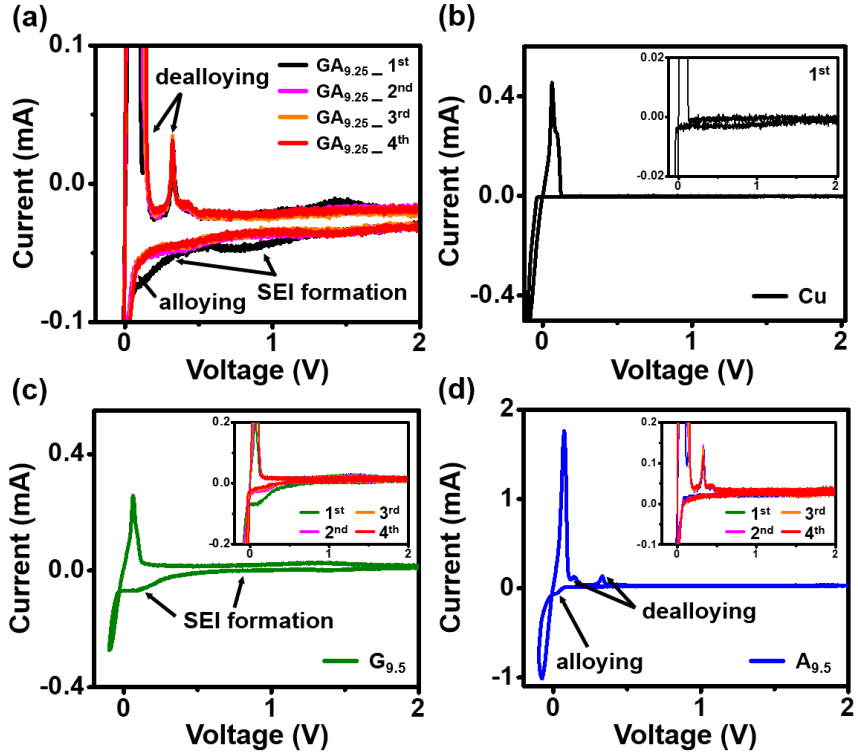

Figure S8. CV curves of half cells of (a) several cycles of $GA_{9.25}$, first cycles of (b) Cu (inset: enlarged view of CV curves), (c) $G_{9.5}$, and (d) $A_{9.5}$ electrodes measured at a scan rate of 0.1 mV/s (inset: several cycles of CV curves).

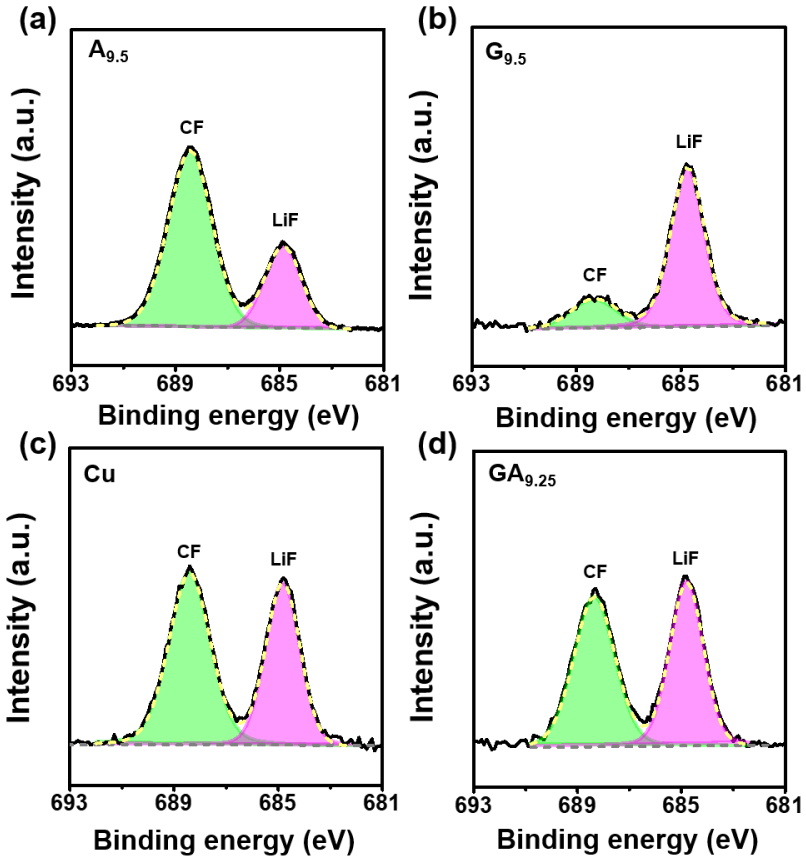

Figure S9. XPS spectra of F 1s peaks in SEI layer formed on (a) $A_{9.5}$, (b) $G_{9.5}$, (c) Cu, and (d) $GA_{9.25}$ after ten cycles in 1 M LiTFSI in DOL/DME with 1 wt% $LiNO_3$ electrolyte.

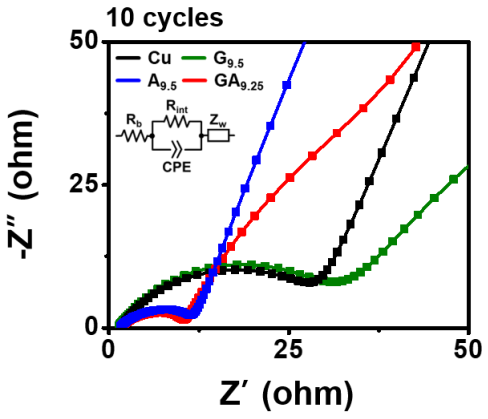

Figure S10. EIS of half cells with Cu, $G_{9.5}$, $A_{9.5}$, and $GA_{9.25}$ after 10 cycles with 1 wt% $LiNO_3$ additive in DOL/DME (1:1) electrolytes.

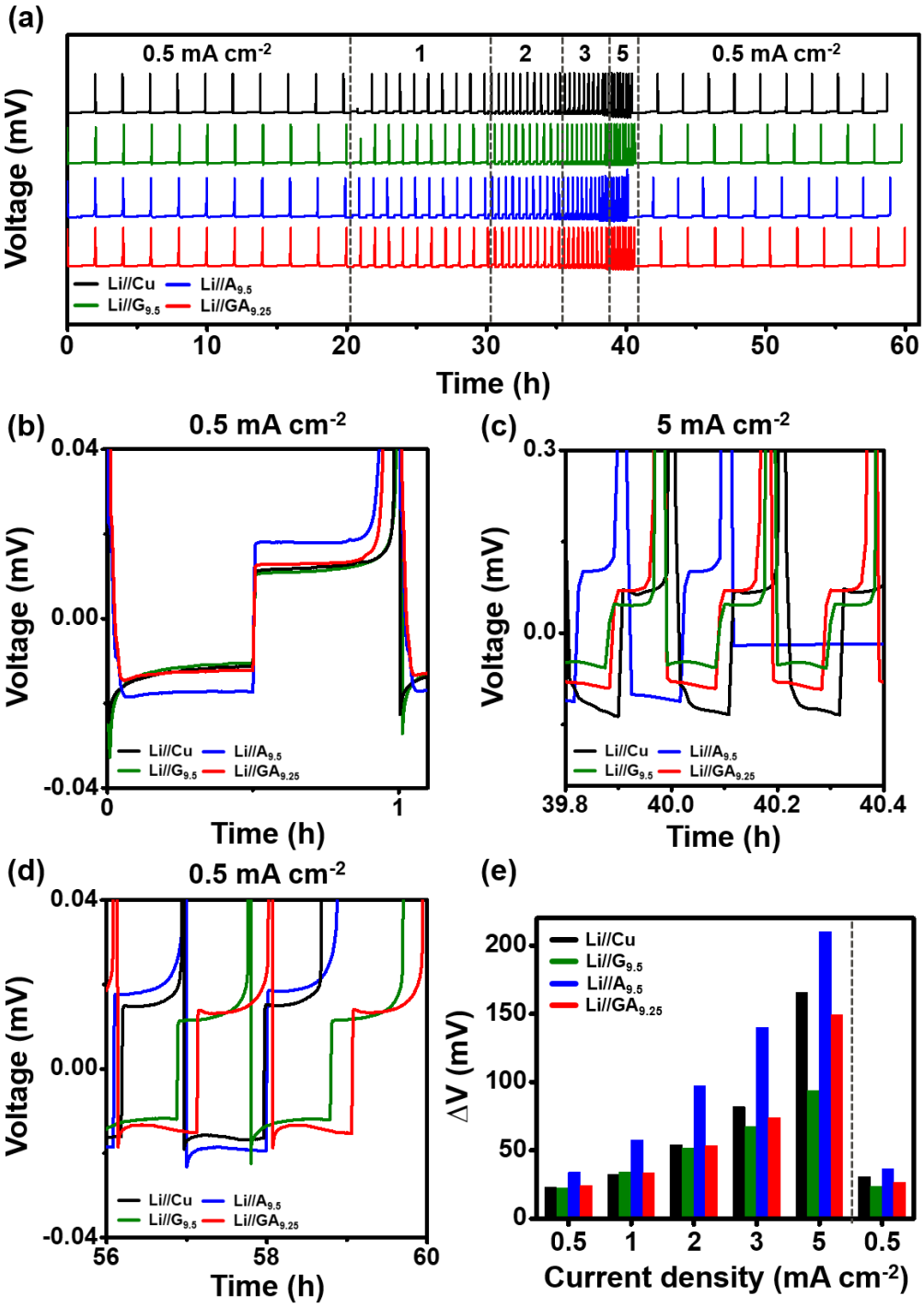

Figure S11. (a) Rate performances of half cells with Cu, $G_{9.5}$, $A_{9.5}$, and $GA_{9.25}$ at various current densities from 0.5 to 5 mA cm^{-2} with a fixed capacity of 0.5 mAh cm^{-2}, for 10 cycles at each step. Enlarged view of voltage curves (b) at 0.5 mA cm^{-2}, (c) 5 mA cm^{-2}, (d) at return to 0.5 mA cm^{-2}. (e) Overvoltage values for each current density of Cu, $G_{9.5}$, $A_{9.5}$ and $GA_{9.25}$.

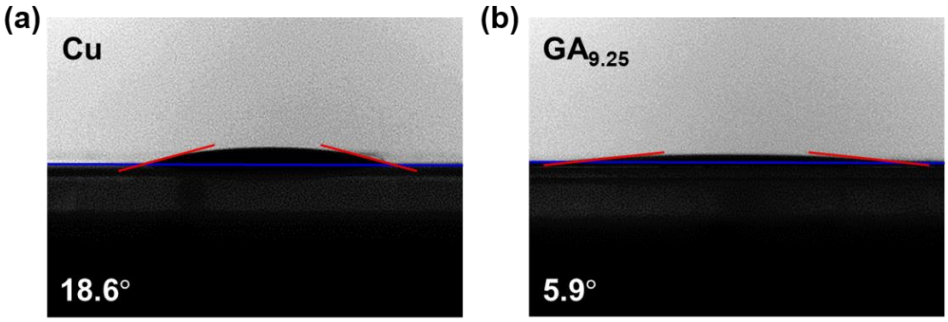

Figure S12. Contact angles of (a) Cu and (b) $GA_{9.25}$ with liquid electrolytes of 1 M LiTFSI in DOL/DME (1:1) with 1 wt% $LiNO_3$ additives.

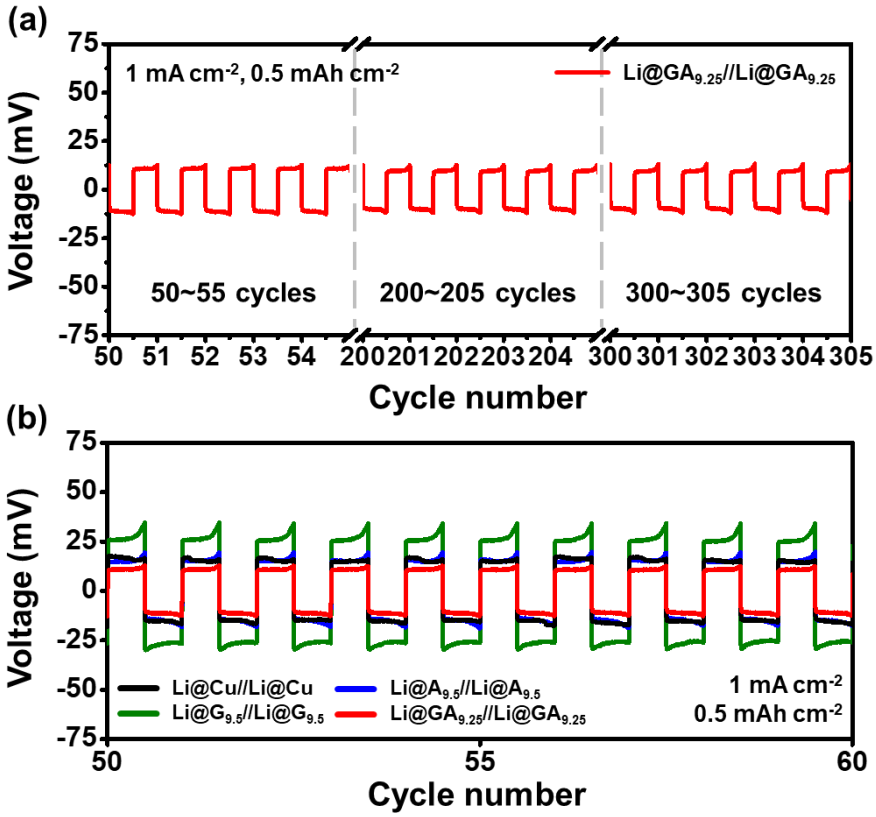

Figure S13. Stable performance of symmetric cells with 2 mAh cm^{-2} of Li pre-deposited on samples as obtained from Figure 7e (a) $Li@GA_{9.25}$ symmetric cells over five cycles and (b) closer view from 50 to 60 cycles (test at 1 mA cm^{-2}, 0.5 mAh cm^{-2}).

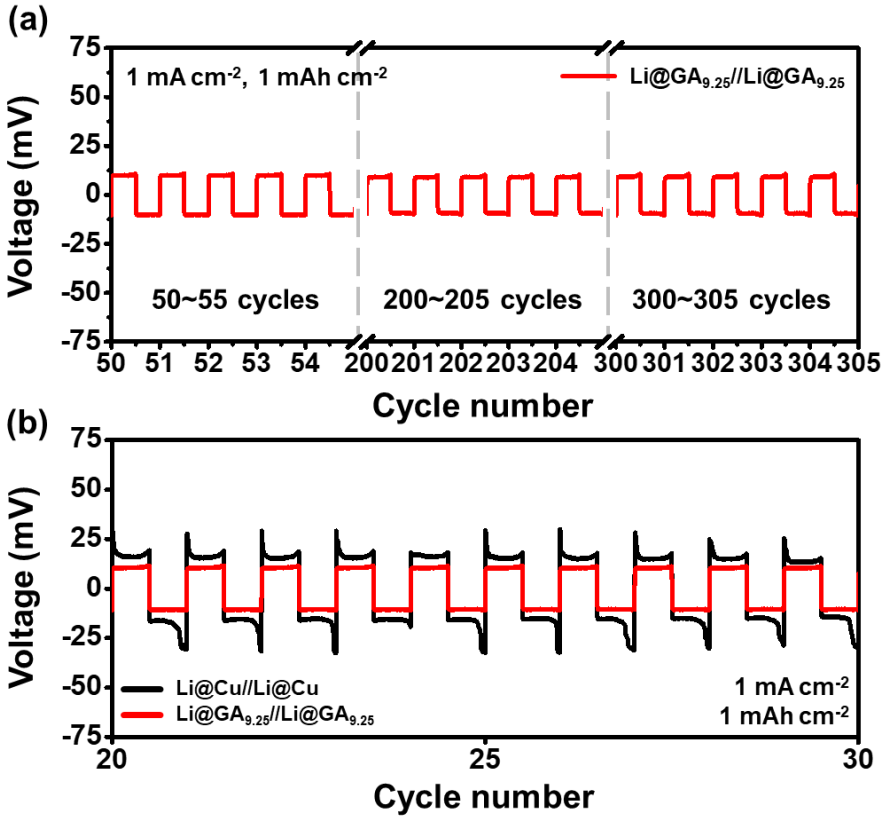

Figure S14. Stable performance of symmetric cells with 4 mAh cm^{-2} of Li pre-deposited on samples as obtained from Figure 7f (a) $Li@GA_{9.25}$ symmetric cells over five cycles and (b) closer view from 20 to 30 cycles (test at 1 mA cm^{-2}, 1 mAh cm^{-2}).

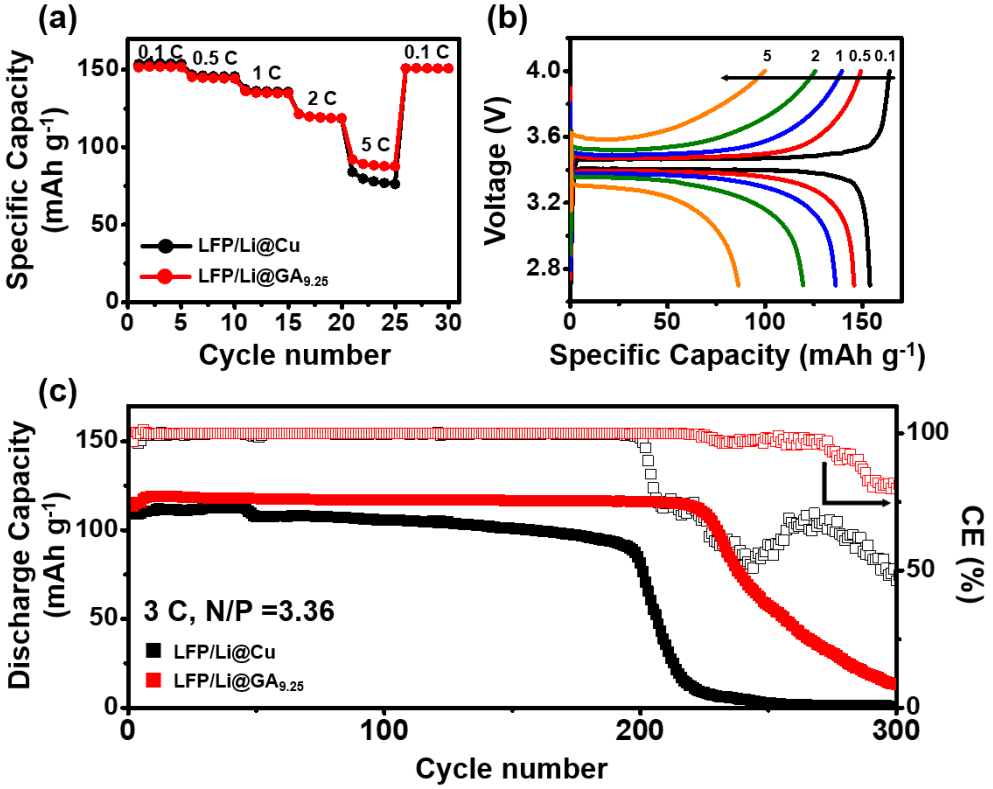

Figure S15. (a) Rate performances of full cells after Li plating with 4 mAh cm^{-2} at various current rates from 0.1 to 5 C compared with LFP/Li@Cu, and LFP/Li@$GA_{9.25}$. (b) Charge/discharge curves of LFP/Li@$GA_{9.25}$ full cell at various current rates. (c) Cycle performance and Coulombic efficiency of LFP/Li@Cu, and LFP/Li@$GA_{9.25}$ full cells after Li plating with a capacity of 4 mAh cm^{-2} at 3 C.

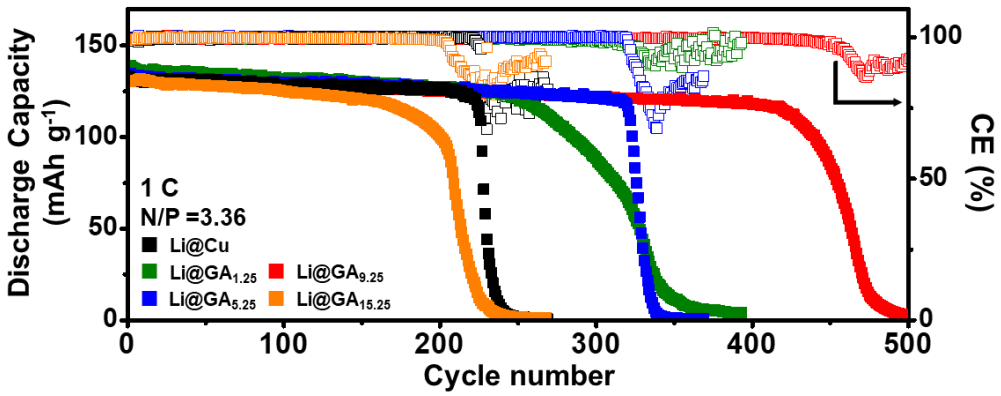

Figure S16. Cycle performance and Coulombic efficiency of LFP/Li@$GA_{n.25}$ full cells according to the number of quadruple layers after Li plating with 4 mAh cm^{-2} capacity at 1 C.

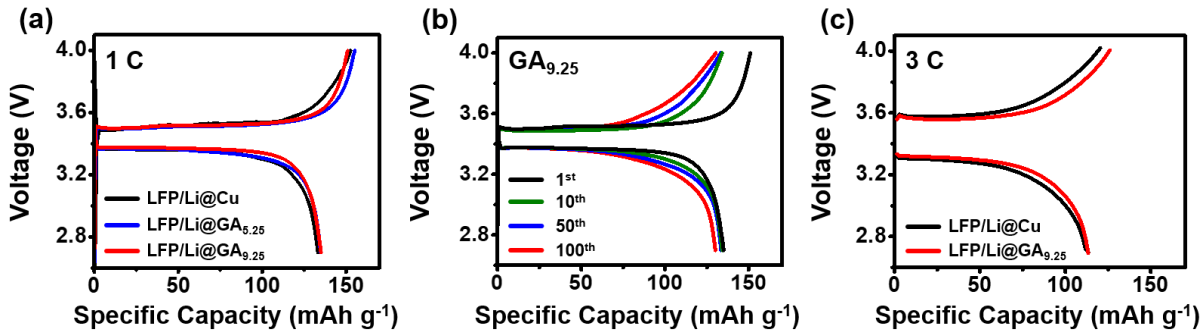

Figure S17. (a) Charge/discharge curves in first cycle of LFP/Li@Cu, LFP/Li@$GA_{5.25}$, and LFP/Li@$GA_{9.25}$ full cells at 1 C. (b) Charge/discharge curves of LFP/Li@$GA_{9.25}$ full cells at 1^{st}, 10^{th}, 50^{th}, and 100^{th} cycles. (c) Charge/discharge curves in the first cycle of LFP/Li@Cu and LFP/Li@$GA_{9.25}$ full cells at 3 C. All samples were tested after Li plating with a capacity of 4 mAh cm^{-2}, as obtained from Figure 9c–d.

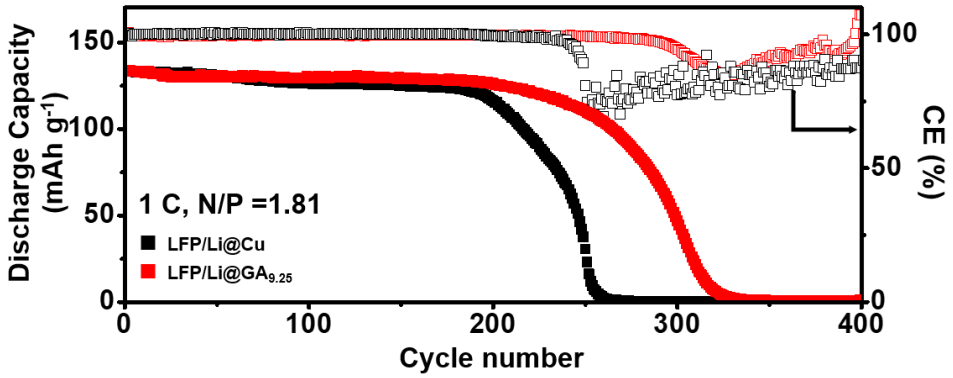

Figure S18. Cycle performance and Coulombic efficiency of LFP/Li@Cu, and LFP/Li@$GA_{9.25}$ full cells after Li plating with a capacity of 2 mAh cm^{-2} at 1 C.

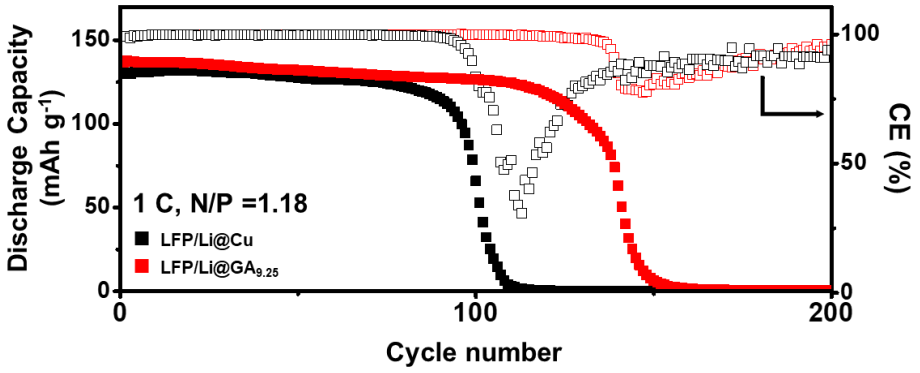

Figure S19. Cycle performance and Coulombic efficiency of LFP/Li@Cu, and LFP/Li@$GA_{9.25}$ full cells after Li plating with a capacity of 2 mAh cm^{-2} at 1 C with high cathode mass loading (10 mg cm^{-2}).

References

[S1] C. Yang, H. Gu, W. Lin, M. M. Yuen, C. P. Wong, M. Xiong, B. Gao, *Adv. Mater.* **2011**, *23*, 3052.

[S2] C. Kim, H. An, A. Jung, B. Yeom, *J. Colloid Interface Sci.* **2017**, *493*, 371.

[S3] Q. Chen, Y. Wei, X. Zhang, Z. Yang, F. Wang, W. Liu, J. Zuo, X. Gu, Y. Yao, X. Wang, F. Zhao, S. Yang, Y. Gong, *Adv. Energy Mater.* **2022**, *12*, 2200072.

[S4] J. Jiang, X. Hu, S. Lu, C. Shen, S. Huang, X. Liu, Y. Jiang, J. Zhang, B. Zhao, *Energy Storage Mater.* **2023**, *54*, 885.

[S5] R. He, Y. Wang, C. Zhang, Z. Liu, P. He, X. Hong, R. Yu, Y. Zhao, J. Wu, L. Zhou, L. Mai, *Adv. Energy Mater.* **2023**, *13*, 2204075.

[S6] S. Q. Li, L. Zhang, T. T. Liu, Y. W. Zhang, C. Guo, Y. Wang, F. H. Du, *Adv. Mater.* **2022**, *34*, 2201801.

[S7] J. Ma, J. Yang, C. Wu, M. Huang, J. Zhu, W. Zeng, L. Li, P. Li, X. Zhao, F. Qiao, Z. Zhang, D. He, S. Mu, *Energy Storage Mater.* **2023**, *56*, 572.

[S8] Y. Jin, I. H. Lee, T. Gu, S. H. Jung, H. Chang, B. S. Kim, J. Moon, D. Whang, *Adv. Funct. Mater.* **2024**, *34*, 2310097.

[S9] Z. Hou, Y. Yu, W. Wang, X. Zhao, Q. Di, Q. Chen, W. Chen, Y. Liu, Z. Quan, *ACS Appl. Mater. Interfaces* **2019**, *11*, 8148.

[S10] Y. Fang, S. L. Zhang, Z. P. Wu, D. Luan, X. W. Lou, *Sci. Adv.* **2021**, *7*, eabg3626.

[S11] C. Gao, J. Li, K. Sun, H. Li, B. Hong, M. Bai, K. Zhang, Z. Zhang, Y. Lai, *Chem. Eng. J.* **2021**, *412*, 128721.

[S12] J. Gu, Q. Zhu, Y. Shi, H. Chen, D. Zhang, Z. Du, S. Yang, *ACS Nano* **2020**, *14*, 891.